

# Circular holographic video display system

Fahri Yaraş,<sup>1,\*</sup> Hoonjong Kang,<sup>1,2</sup> and Levent Onural<sup>1</sup>

<sup>1</sup>Department of Electrical and Electronics Engineering, Bilkent University  
TR-06800 Ankara, Turkey

<sup>2</sup>Realistic Media Platform Research Center, Korea Electronics Technology Institute, #1599,  
Sangam-dong, Mapo-gu, Seoul, 121-835, South Korea

[\\*fahri@ee.bilkent.edu.tr](mailto:fahri@ee.bilkent.edu.tr)

**Abstract:** A circular holographic video display system reconstructs holographic video. Phase-only spatial light modulators are tiled in a circular configuration in order to increase the field of view. A beam-splitter is used to align the active area of the SLMs side by side without any gap. With the help of this configuration observers can see 3D ghost-like image floating in space and can move and rotate around the object. The 3D reconstructions can be observed binocularly. Experimental results are satisfactory.

© 2011 Optical Society of America

**OCIS codes:** (090.2870) Holographic display; (090.1995) Digital holography; (090.4220) Multiplex holography.

---

## References and links

1. M. Kovachev, R. Ilieva, P. Benzie, G.B. Esmer, L. Onural, J. Watson, and T. Reyhan, "Holographic 3DTV displays using spatial light modulators," in *Three-Dimensional Television - Capture, Transmission, Display*, H. Ozaktas and L. Onural, eds., pp. 529–555, (Springer, 2008).
2. F. Yaraş, H. Kang, and L. Onural, "Real-time phase-only color holographic video display system using LED illumination," *Appl. Opt.* **48**(34), H48–H53 (2009).
3. M. Paturzo, P. Memmolo, A. Finizio, R. Nsnen, T. Naughton, and P. Ferraro, "Synthesis and display of dynamic holographic 3D scenes with real-world objects," *Opt. Express* **18**, 8806–8815 (2010).
4. L. Onural, F. Yaraş and H. Kang, "Digital holographic three-dimensional video displays," *Proc. IEEE* **99**(4), 576–589 (2011).
5. T. Kozacki, "On resolution and viewing of holographic image generated by 3D holographic display," *Opt. Express* **18**, 27118–27129 (2010).
6. F. Yaraş, H. Kang, and L. Onural, "Multi-SLM holographic display system with planar configuration," *3DTV-Conference: The True Vision - Capture, Transmission and Display of 3D Video (3DTV-CON)*, 2010.
7. F. Yaraş, H. Kang, and L. Onural, "State of the art in holographic displays: a survey," *J. Disp. Technol.* **6**(10), 443–454 (2010).
8. Holoeye Photonics AG, <http://www.holoeye.com/>.
9. J. W. Goodman, *Introduction to Fourier Optics* (McGraw-Hill, 1996).
10. N. Fukaya, K. Maeno, O. Nishikawa, K. Matumoto, K. Sato, and T. Honda, "Expansion of the image size and viewing zone in holographic display using liquid crystal devices," *Proc. SPIE* **2406**, 283–289 (1995).
11. C. Slinger, P. Brett, V. Hui, G. Monnington, D. Pain, and I. Sage, "Electrically controllable multiple, active, computer-generated hologram," *Opt. Lett.* **22**(14), 1113–1115 (1997).
12. M. Stanley, R. W. Bannister, C. D. Cameron, S. D. Coomber, I. G. Cresswell, J. R. Hughes, V. Hui, P. O. Jackson, K. A. Milham, R. J. Miller, D. A. Payne, J. Quarrel, D. C. Scattergood, A. P. Smith, M. A. G. Smith, D. L. Tipton, P. J. Watson, P. J. Webber, and C. W. Slinger, "100-megapixel computer-generated holographic images from active tiling: a dynamic and scalable electro-optic modulator system," *Proc. SPIE* **5005**, 247–258 (2003).
13. J. Hahn, H. Kim, Y. Lim, G. Park, and B. Lee, "Wide viewing angle dynamic holographic stereogram with a curved array of spatial light modulators," *Opt. Express* **16**(16), 12372–12386 (2008).
14. D. Palima and V. Daria, "Holographic projection of arbitrary light patterns with a suppressed zero-order beam," *Appl. Opt.* **46**, 4197–4201 (2007).

## 1. Introduction

Spatial light modulators (SLMs) are widely used in holographic display research [1–6]. Liquid crystal devices (LCDs), liquid crystal on silicon SLMs (LCoS), digital micromirror devices (DMDs) are some of the utilized SLM types [7]. In our experiments we used Holoeye HEO-1080P phase-only LCoS SLMs [8]. Those SLMs are easy to use and have  $1920 \times 1080$  pixels. In addition, they have high diffraction efficiency which is defined as the ratio of the power of the diffracted light beam in one order to the power of the incident beam [9]. In spite of those advantages compared to other SLM types, a single SLM is not sufficient for binocular vision; and thus, observers may not see the reconstructions as 3D. One of the main reasons is the narrow viewing angle and this stems from larger SLM pixel periods compared to wavelength of the visible light. Typical pixel period for phase-only SLMs is about  $8\mu\text{m}$  and therefore, for green light ( $\lambda = 532\text{nm}$ ), maximum diffraction angle,  $\theta_{max}$ , is approximately  $\mp 1.9^\circ$ . This severely restricts the field of view and prevents binocular vision; therefore, a state-of-the-art single SLM does not support 3D vision. Furthermore, since the overall size of a SLM is quite small, the reconstructed objects are also small in size. As a result, the observer can not move around the reconstruction and can not observe reconstructed object binocularly when only one SLM is used.

Fukaya *et al.* presented a wide holographic display system [10]. In their system, they use transmission type SLMs and align three of them side by side in a planar configuration by using a beam-splitter. They also utilize a lenticular sheet and discard the vertical parallax. Slinger *et al.* proposed a different tiling scheme to increase the field of view [11, 12]. They use an electrically addressed SLM (EASLM) to drive an optically address SLM (OASLM). They first divide the large hologram into 25 partitions ( $5 \times 5$ ) and then each partition is projected onto the OASLM. Since the size of the OASLM is larger, the observer can see the reconstructed images comfortably. Hahn *et al.* also presented a holographic display system that contains a curved array of SLMs [13]. In their display system, they use 12 SLMs and by using transfer lenses and mirror modules they divide diffracted light emanated from each SLM into three partitions in the form of horizontal strips. And then, they recombine those partitions to obtain a three times wider field. Although the height of the display is three times smaller, effective hologram size along the horizontal direction is three times wider. Their resultant display size is  $36864 \times 256$ . They use an asymmetric diffuser and generate horizontal parallax only holographic reconstructions. With the help of an array of SLMs, the resultant viewing angle was reported as approximately  $22.8^\circ$ .

We propose a novel holographic video display system which uses nine phase-only SLMs placed in a circular configuration. The proposed system has full parallax and observers can see the reconstructions floating in space. In [13], however, the reconstructions do not have vertical parallax. In addition, a novel illumination scheme is used in our proposed system. In order to illuminate all SLMs, we use a cone mirror; and as a result, a single astigmatic wave illuminates all of the SLMs. Such an illumination scheme results in a very convenient setup in terms of alignments and adjustments. However, in [13] each SLM is illuminated by a separate plane wave and relay lenses are used to tile SLMs. We use a beam-splitter to tile the SLMs side by side without any gap between them. Moreover, we use phase-only SLMs in the proposed system. The results show that the quality of the reconstructions is satisfactory.

In Section 2 we define the field of view in holographic displays and investigate the advantages of the circular configuration. In Section 3 the optical setup is presented. Section 4 presents the hologram generation algorithm and the experimental results. Conclusions are drawn in the last section.

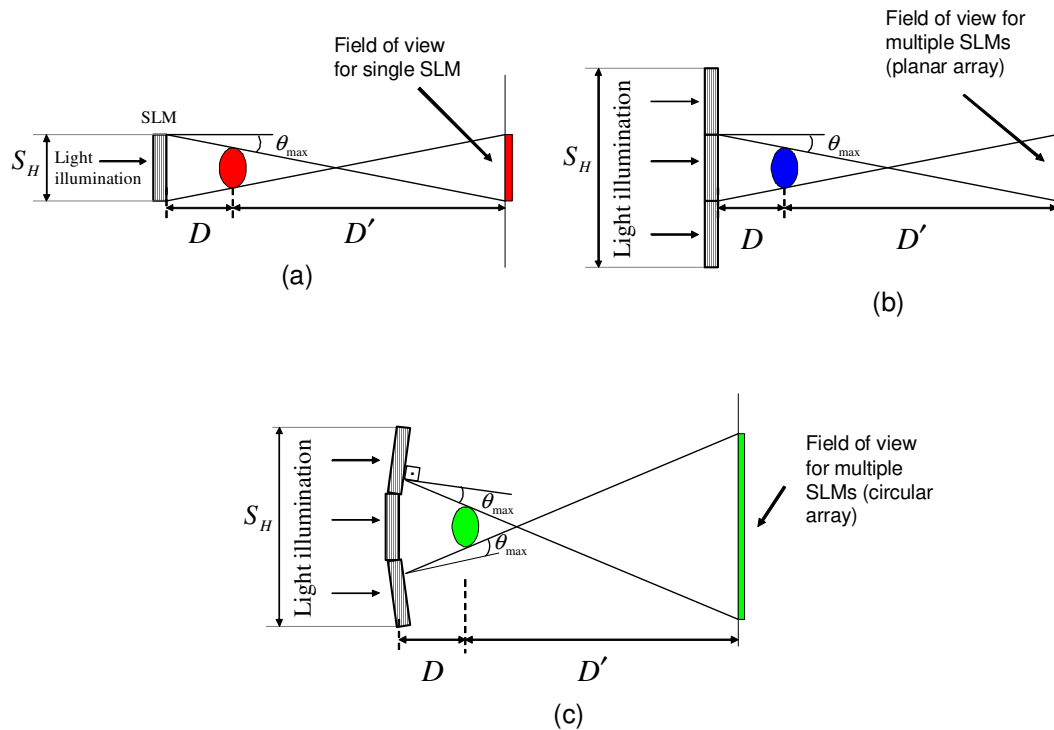


Fig. 1. Field of view for (a) single SLM, (b) multiple SLMs in planar configuration, (c) multiple SLMs in circular configuration.

## 2. Field of view in holographic displays

Field of view is one of the important properties of displays. Commercially available LCD displays (monitors, TVs and so on) have a wide field of view because of the diffused light source at the back of the LCD panel. However, since diffused light sources randomize the phase of the propagating waves, they are not suitable for holographic reconstructions. In order to keep the relative phase of the propagating waves, we need to use somewhat coherent light. In our experiments we use either laser or LED illumination. Appropriate LED illumination also has sufficient coherence for holographic reconstruction purposes [2]. When we use coherent light sources, field of view of the SLMs are restricted by the SLM size and pixel period. For a typical LCoS SLM, the size is about  $1\text{ cm} \times 2\text{ cm}$ , pixel period,  $\Delta_p$ , is about  $8\mu\text{m}$  and the corresponding diffraction angle,  $\theta_{max}$ , is about  $1.9^\circ$  (where  $\Delta_p = \lambda / [2\sin(\theta_{max})]$ ). A more detailed analysis can be found in [4, 6]. Figure 1(a) shows the relation between the field of view, the size and the diffraction angle. Here the field of view denotes an area on the observation plane where the entire object can be seen while the full bandwidth of the SLM is utilized. As we move away from the field of view, either some parts of the reconstructed object will not be visible or the bandwidth used for reconstruction (thus, the quality/sharpness) decreases. Unfortunately, due to the small size of a single SLM and the narrow diffraction angle, the resultant field of view is not sufficient to observe 3D reconstructions comfortably. Figure 1(b) shows that if all parameters are kept as in Fig. 1(a), including the reconstructed object size, using multiple SLMs in a planar configuration does not bring any improvement in terms of the field of view compared to the single SLM case. Note that, full bandwidth of only the middle SLM is used for the reconstruction and there is no contribution from other SLMs to such a reconstruction. Meanwhile,

for illustration purposes, it is assumed that there is no mount around the active area of the SLM; and therefore, there is no gap between the SLMs when they are concatenated side by side. In order to increase the field of view, we propose to have a circular (curved) holographic display. As shown in Fig. 1(c), with the help of a circular configuration, the field view increases significantly. With this arrangement we expect to have a better 3D perception in holographic displays since the observer can see the reconstruction binocularly and also rotate around it within the field of view.

### 3. Optical setup

As mentioned above, SLMs are tiled in a circular configuration to increase the field of view. However, commercially available SLMs have frames (see Fig. 2(a)); therefore, the resultant field of view becomes discontinuous (see Fig. 2(b)). This eventually decreases the quality of 3D perception. In order to overcome this problem, we propose to use a beam splitter (half-mirror) as in [6, 10]. Figure 3 shows the schematic of the experimental setup. The beam splitter is used to align SLMs' active areas without any gap between them. However this alignment is virtual, which means SLMs that are on one side of the beam splitter are imaged onto the other side. A beam splitter is used to eliminate the gap between SLMs also in the holographic display systems reported in [6, 10]. We use a cone mirror to direct incoming light toward all SLMs. Due to the shape of the cone mirror, radius of curvatures of the illuminating light beam in vertical and horizontal axes may not be equal (see Fig. 4(a)). As seen in Fig. 4(b), vertical and horizontal illumination waves are originating from different positions on the optical axis. The effect of this non-symmetric illumination is canceled out during the hologram generation step as a consequence of a multiplication by a correction term so that the reconstructed wave propagates as if the original hologram is illuminated by a plane wave. Expressions for vertical and horizontal illumination waves are presented in Section 4. Figure 5 shows the photographs of the optical setup. Figure 5(a) shows the alignment of the SLMs and SLM modules. Side view of the setup and the cone mirror can be seen in Fig. 5(b) and Fig. 5(c), respectively. Resultant continuous array of SLMs can also be seen in Fig. 5(b). Fig. 5(d) shows the SLMs and the beam-splitter together. SLMs are tilted up a little to position the reconstructed 3D object slightly above the setup (See Fig. 4(a)). Otherwise components may block the observer's vision. Based on our experiments and subjective test results, we observed that there is a negligible reduction in the quality of the reconstructions for a tilted illumination of up to  $20^\circ$ .

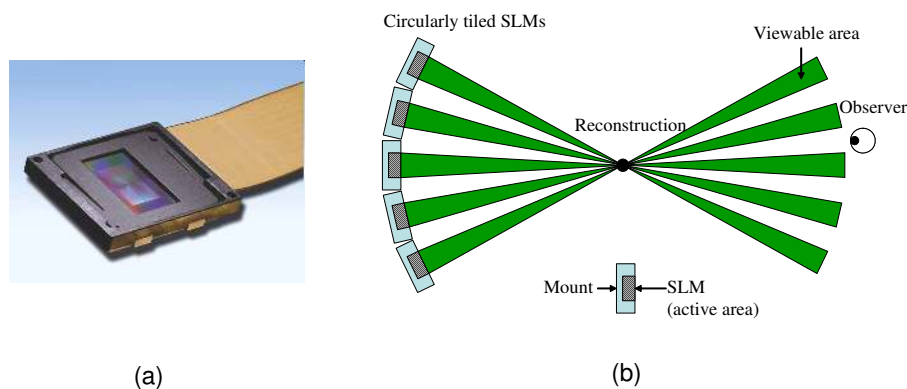


Fig. 2. (a) Picture of a LCoS SLM produced by HOLOEYE [8] (b) Discontinuous field of view due the frame.

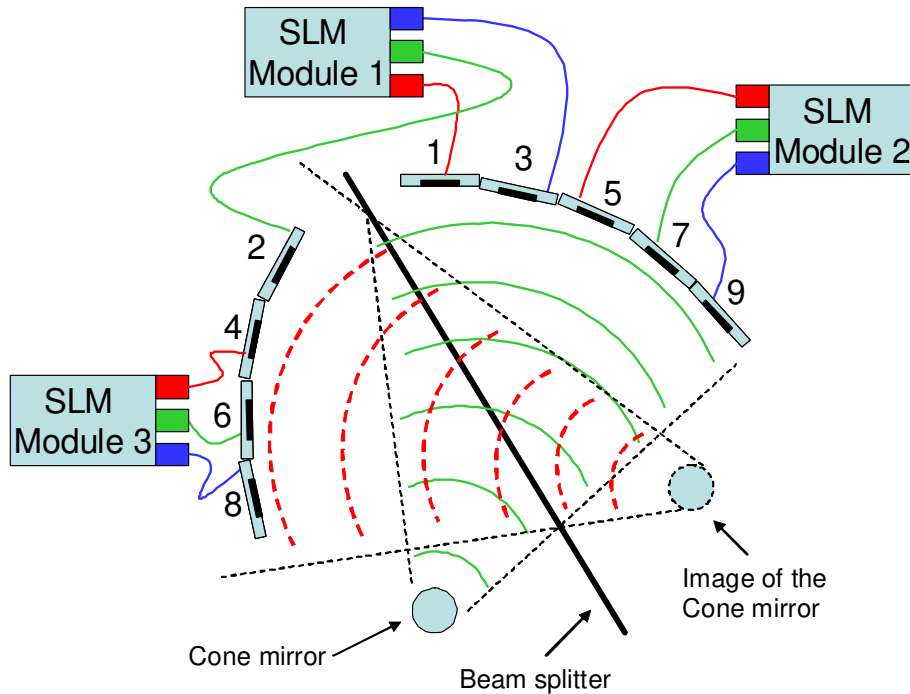


Fig. 3. Top view of the experimental setup.

#### 4. Hologram generation and experimental results

In our holographic video display system, we use a computer generated holographic video of a three-dimensional computer graphic model of a horse. Figure 6 shows the picture of the model at an instant. The model is a 3D point cloud object. The original video contains 24 frames and we are able to extract 3D point cloud data for each frame. Once we have the point cloud data for a frame, we can calculate a hologram of the model for any viewing position. In our case, we calculate nine holograms for each frame for nine different viewing positions with an angular separation of  $3^\circ$  along the horizontal direction. Hologram generation algorithm is presented in the next paragraph. As shown in Fig. 3, we use three SLM modules. Each module has three phase-only SLMs. Drivers of the modules are originally designed for conventional 2D color video operation (RGB). However, we use all such channels for our monochromatic holographic display. In order to have an efficient interface between the computer and the display we grouped and assigned the driver channels to our SLMs as shown in Fig. 3. Those nine holograms are first grouped for the driver modules, as shown in Fig. 7. Then they are written in a single RGB bitmap image of size  $(3 \times M)$  by  $N$  where  $(M, N) = (1920, 1080)$  is the single SLM size. This procedure is applied for each frame of the video.

We start by describing the hologram computation for one of the nine SLMs. Let  $(\xi, \eta)$  describe the hologram (SLM) plane. In order to calculate the holograms, we extracted the point cloud data from the three-dimensional computer graphic model. Each point in the point cloud has a complex amplitude denoted as  $O(x, y, z) = o(x, y, z) \exp(j\theta_o(x, y, z))$ , where  $o(x, y, z)$  and  $\theta_o(x, y, z)$  denote the magnitude and the phase of the object wave at the object point, respectively. As mentioned in the previous section, expanding non-symmetric wave is used to illuminate the holograms. Therefore, a correction term is required to compensate for this effect while

computing the holograms. This illuminating wave can be expressed as a separable function. In the horizontal direction, the incoming wave is reflected radially by the cone mirror. Therefore, the center of the horizontal spherical wave is at the center of the cone mirror. As shown in Fig. 4, the distance between the SLM and the center of the cone mirror is denoted as  $D_l$ . The illuminating wave along the horizontal direction,  $P(\xi)$ , is given approximately as,

$$P(\xi) = \exp\left(jk\frac{\xi^2}{2D_l}\right), \quad (1)$$

since our SLM sizes are small and thus the paraxial approximation is valid. In the vertical direction, the cone mirror behaves just as a slanted mirror. Therefore, it does not change the center of the incoming light. However, since the size of the cone mirror is smaller than the size of the SLM; therefore, we use an expanding illuminating wave along the vertical direction. In this case, the distance between the center of the expanding illuminating wave and the SLM is calculated as  $D_p + D_l$  (See Fig. 4). Thus, the illuminating wave along the vertical direction,  $P(\eta)$ , is given by:

$$P(\eta) = \exp\left(jk\frac{(\eta + S_H/2)^2}{2(D_p + D_l)}\right), \quad (2)$$

where,  $S_H$  is the height of the SLM and  $D_p$  is the distance between the cone mirror and the center of the spherical illumination wave. Furthermore, as a typical property of the SLMs, a strong undiffracted beam exists at the reconstructions [14]. There are several methods to eliminate this effect. We use off-axis holograms to separate reconstruction from undiffracted beam. We apply an additional carrier frequency along the vertical direction for this purpose. We can insert this term,  $P_t$ , also to the correction term and it is given by:

$$P_t(\eta) = \exp(jk\eta \sin(\theta_t)), \quad (3)$$

where,  $\sin(\theta_t)$  is the angle between undiffracted beam and the reconstructed beam. As a result, the overall correction term becomes:

$$P(\xi, \eta) = \exp\left(jk\frac{\xi^2}{2D_l}\right) \exp\left(jk\frac{(\eta + S_H/2)^2}{2(D_p + D_l)} + jk\eta \sin(\theta_t)\right). \quad (4)$$

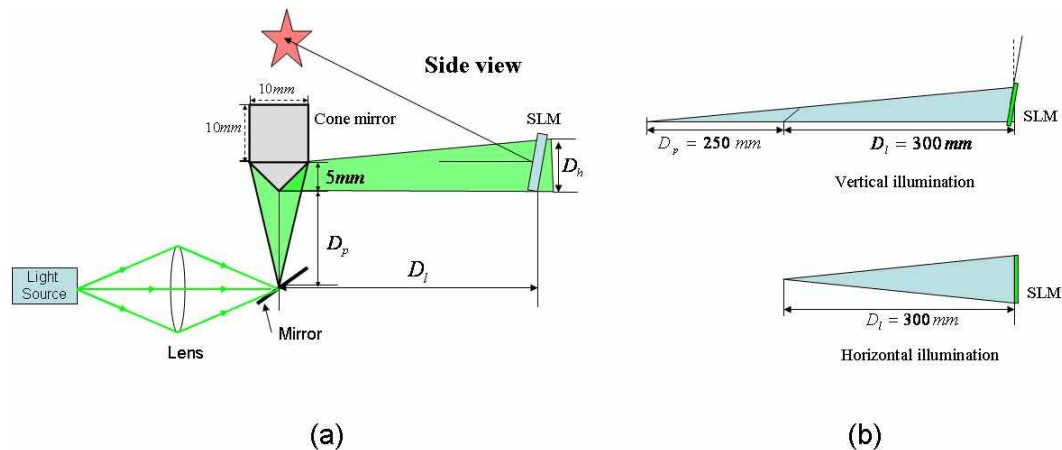


Fig. 4. (a) Side view of the experimental setup. (b) Vertical and horizontal illumination.



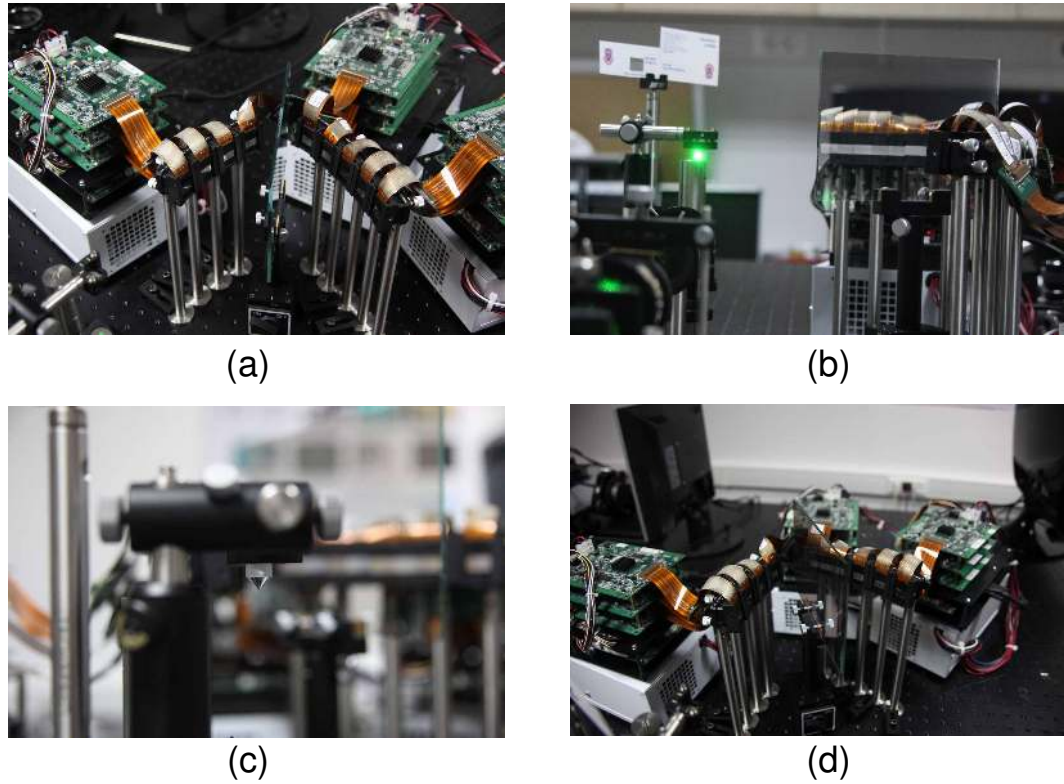


Fig. 5. Pictures of (a) SLMs and SLM Modules, (b) side view of the setup, (c) cone mirror and (d) SLMs and beam splitter.

Digital holograms are calculated based on a light propagation algorithm by using point cloud data. Our light propagation algorithm is based on Rayleigh-Sommerfeld kernel which gives exact light propagation expression for scalar diffraction [9]. The Rayleigh-Sommerfeld diffraction for the point cloud data at larger distances (no evanescent waves) yields:

$$S(\xi, \eta) = \sum_{p=1}^N O(x_p, y_p, z_p) \frac{\exp(jkr_p)}{r_p} \quad , \quad (5)$$

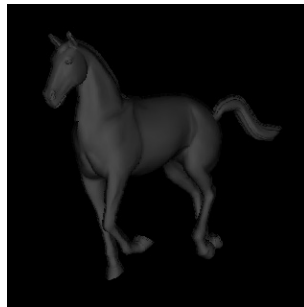


Fig. 6. Single frame of the video of the 3D horse model (courtesy of [www.sharecg.com](http://www.sharecg.com)).

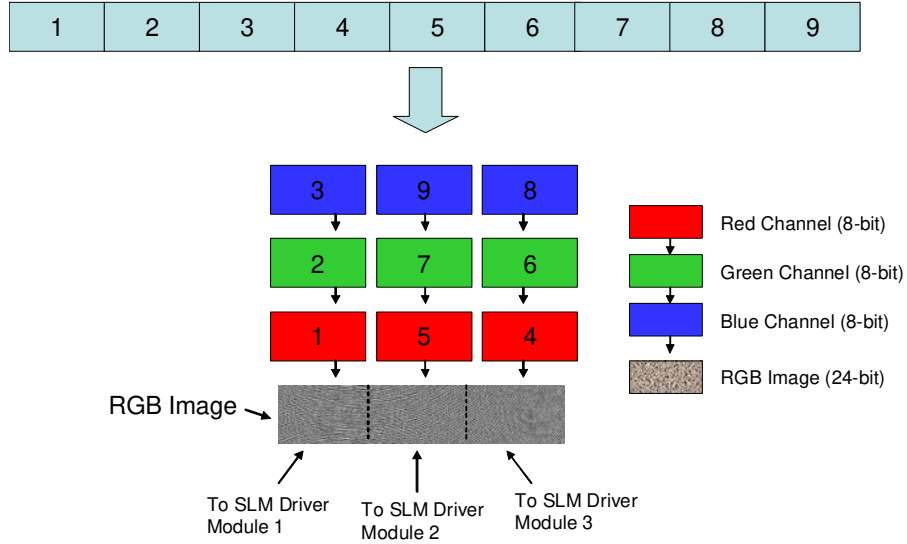


Fig. 7. Writing nine holograms on a single bitmap image.

where,  $N$  is the number of points in the point cloud of the three-dimensional computer graphic model,  $p$  is the index of the points,  $k$  is the wavenumber ( $k = 2\pi/\lambda$ , where  $\lambda$  is the wavelength) and  $r_p$  is the distance between  $p^{th}$  point and the hologram plane and given as:

$$r_p = [(\xi - x_p)^2 + (\eta - y_p)^2 + z_p^2]^{1/2} . \quad (6)$$

After multiplying by the correction term, the complex field on the hologram plane ( $\xi, \eta$  plane) becomes:

$$G(\xi, \eta) = P(\xi, \eta) \sum_{p=1}^N O(x_p, y_p, z_p) \frac{\exp(jkr_p)}{r_p} . \quad (7)$$

Then, the pixelated complex field on the hologram plane is calculated as:

$$g(m, n) \triangleq G\left(\left(m - \frac{(M+1)}{2}\right)\Delta_m, \left(n - \frac{(N+1)}{2}\right)\Delta_n\right) , \quad m \in [1, 1920] \text{ and } n \in [1, 1080]. \quad (8)$$

Here  $M$  and  $N$  are number of columns and rows of the pixelated complex field, respectively; and,  $\Delta_m$  and  $\Delta_n$  are pixel periods along the corresponding directions. Since our SLMs are phase-only, we discard the magnitude and take only the phase information of the complex field. Of course, if full complex field is used, the reconstruction quality will be better. Discarding the magnitude of a complex field is a non-linear process and will degrade the quality of the reconstructions. Edges may be enhanced and the intensity in smooth areas may be suppressed. However, based on our subjective tests we observed that when only the phase information is used, the quality of the reconstructions is still satisfactory for a causal observer. Since our SLMs have  $1920 \times 1080$  pixels,  $M = 1920$  and  $N = 1080$ .

The computation procedure described above is repeated for each one of the nine SLMs by revising the ( $\xi, \eta$ ) plane and the relative coordinates, ( $x_p, y_p, z_p$ ), of the object points to match the SLM position.

Optical reconstructions for a single frame for three different angles are shown in Fig. 8. The distance between the center of the cone mirror and the SLM,  $D_l$ , is  $0.3m$ , and the distance



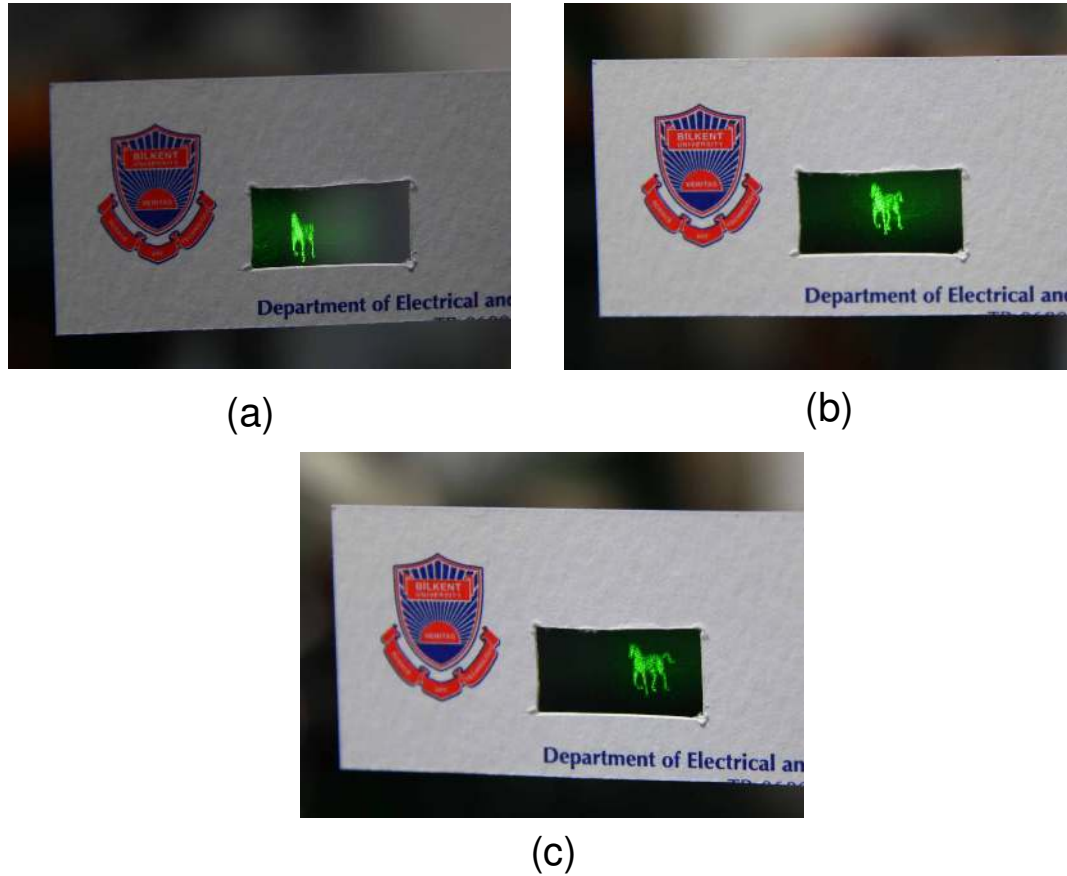


Fig. 8. (Media 1) Optical reconstructions for a single frame for (a) 0 degree, (b) 12 degrees and (c) 24 degrees. (The business card with the rectangular aperture is placed both as a size reference and to block distracting optical component views.)

between the center of the illuminating wave and the SLM,  $D_p + D_l$ , is  $0.55m$ . The reconstruction distance is about  $0.35m$  and the height of the reconstruction is approximately  $1cm$ . We use green laser ( $\lambda = 532nm$ ) for video reconstruction. LED illumination can be used for naked eye observation. Total field of view is approximately  $24^\circ$  and this gives a quite comfortable range for an observer to move around the reconstruction.

## 5. Conclusion

SLMs are commonly used in holographic display systems due to their desirable features. However, small size and narrow diffraction angle limit the field of view, and thus the 3D vision, when a single SLM is used. In order to overcome this problem, we proposed a novel circular multi-SLM holographic display system. As a consequence of this new design we were able to increase the size and the field of view; this gives the observer a freedom within a larger range and thus yields a more comfortable 3D vision. Laser illumination is replaced by LED illumination to assume safety for naked eye observation. Observers can see the reconstructed 3D objects floating in space binocularly. Experimental results are satisfactory and the system can be used as a holographic video display.

### **Acknowledgment**

This work is supported by EC within FP7 under Grant 216105 with the acronym Real 3D. Dr. H. Kang was with Bilkent University, Turkey, when this work was conducted. He is now with Korea Electronics Technology Institute (KETI), South Korea.